Mass Spectrometry and Theoretical Studies on N–C Bond Cleavages in the N-Sulfonylamidino Thymine Derivatives

ARTICLE *in* JOURNAL OF THE AMERICAN SOCIETY FOR MASS SPECTROMETRY · MARCH 2015

Impact Factor: 2.95 · DOI: 10.1007/s13361-014-1068-8 · Source: PubMed

J. Am. Soc. Mass Spectrom. (2015) 26:833–842
DOI: 10.1007/s13361-014-1068-8

RESEARCH ARTICLE

Mass Spectrometry and Theoretical Studies on N–C Bond Cleavages in the *N*-Sulfonylamidino Thymine Derivatives

Renata Kobetić,[1] Snježana Kazazić,[2] Borislav Kovačević,[3] Zoran Glasovac,[4] Luka Krstulović,[5] Miroslav Bajić,[5] Biserka Žinić[1]

[1]Laboratory of Supramolecular and Nucleoside Chemistry, Division of Organic Chemistry and Biochemistry, Ruđer Bošković Institute, 10000, Zagreb, Croatia
[2]Laboratory for Chemical Kinetics and Atmospheric Chemistry, Division of Physical Chemistry, Ruđer Bošković Institute, 10000, Zagreb, Croatia
[3]Group for Quantum Organic Chemistry, Division of Organic Chemistry and Biochemistry, Ruđer Bošković Institute, 10000, Zagreb, Croatia
[4]Laboratory for Physical-organic Chemistry, Division of Organic Chemistry and Biochemistry, Ruđer Bošković Institute, 10000, Zagreb, Croatia
[5]Department of Chemistry and Biochemistry, Faculty of Veterinary Medicine, University of Zagreb, 10000, Zagreb, Croatia

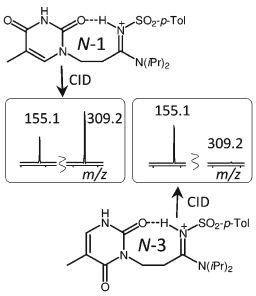

Abstract. The reactivity of new biologically active thymine derivatives substituted with 2-(arylsulfonamidino)ethyl group at N1 and N3 position was investigated in the gas phase using CID experiments (ESI-MS/MS) and by density functional theory (DFT) calculations. Both derivatives show similar chemistry in the negative mode with a retro-Michael addition (Path A) being the most abundant reaction channel, which correlate well with the fluoride induced retro-Michael addition observed in solution. The difference in the fragmentation of *N*-3 substituted thymine **5** and *N*-1 substituted thymine **1** in the positive mode relates to the preferred cleavage of the sulfonyl group (*m/z* 155, Path B) in *N*-3 isomer and the formation of the acryl sulfonamidine **3** (*m/z* 309) via Path A in *N*-1 isomer. Mechanistic studies of the cleavage reaction conducted by DFT calculations give the trend of the calculated activation energies that agree well with the experimental observations. A mechanism of the retro-Michael reaction was interpreted as a McLafferty type of fragmentation, which includes H_β proton shift to one of the neighboring oxygen atoms in a 1,5-fashion inducing N1(N3)–C_α bond scission. This mechanism was found to be kinetically favorable over other tested mechanisms. Significant difference in the observed fragmentation pattern of *N*-1 and *N*-3 isomers proves the ESI-MS/MS technique as an excellent method for tracking the fate of similar sulfonamidine drugs. Also, the observed *N*-1 and/or *N*-3 thymine alkylation with in situ formed reactive acryl sulfonamidine **3** as a Michael acceptor may open interesting possibilities for the preparation of other *N*-3 substituted pyrimidines.

Key words: *N*-sulfonylamidines, Thymine, Retro-Michael addition, ESI-MS, DFT calculations

Received: 23 October 2014/Revised: 10 December 2014/Accepted: 12 December 2014/Published online: 12 March 2015

Introduction

We have recently shown that *N*-sulfonylpyrimidine derivatives of type **I** (Figure 1) possess strong antitumor activity under in vitro [1, 2] and in vivo conditions [3, 4]. To further explore the biological potential of these types of molecules, their structure was modified by combining them with another potent anticancer pharmacophore—the amidine. The amidine group is present in many compounds capable of interacting with a wide range of biological targets [5], resulting in anti-degenerative [6], anticancer [7, 8] and antimicrobial activities [9]. These findings encouraged us to explore the synthesis and chemistry of novel *N*-sulfonylamidino derivatives containing pyrimidine moiety **II** (Figure 1) and to study their biological properties [10].

Electronic supplementary material The online version of this article (doi:10.1007/s13361-014-1068-8) contains supplementary material, which is available to authorized users.

Correspondence to: Borislav Kovačević; *e-mail:* boris@irb.hr, Zoran Glasovac; *e-mail:* glasovac@irb.hr, Biserka Žinić; *e-mail:* bzinic@irb.hr

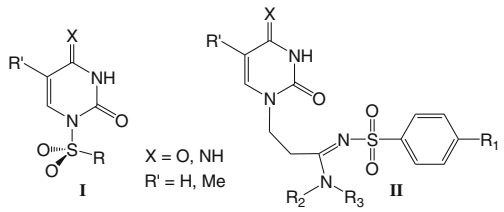

Figure 1. *N*-sulfonylpyrimidine **I** and *N*-sulfonylamidinopyrimidine **II** derivatives

Application of these derivatives as drugs asks for a method that can successfully track the fate of these compounds in organism. HPLC coupled with ESI-MS/MS is often an instrumental technique of choice for this purpose [11, 12], and knowledge of the fragmentation pattern of the starting material is required. Until now, many papers dealing with usual and unusual fragmentation of sulfonamides have been published [13–17], while, to the best of our knowledge, fragmentation of sulfonamidines has not been investigated. Upon CID experiments conducted on simple alkyl-benzenesulfonamides, Attygalle and coworkers noticed a loss of benzenesulfonamide or its protonated form producing alkyl cation or neutral alkene depending on the structure of alkyl substituent [18]. They also observed a low abundance of benzenesulfonyl cation and some other second generation ions. One could assume that these fragments will also appear upon CID experiments conducted on sulfonamidines. Additionally, product ions resulting from the retro-Michael addition of the sulfonamidine **II** are also expected. Several years ago, Walczak and coworkers observed Michael/retro-Michael reaction equilibrium on the *N*-1- and *N*-3-(2-(methylcarboxy)ethyl)thymine under basic conditions [19]. They found significant difference in rates of retro-Michael addition depending on whether substituent is attached to N1 or N3 position of thymine subunit. Thus, the cleavage of C–N1 bond in a retro-Michael reaction occurs under mild conditions, whereas the same reaction starting from *N*-3 substituted derivative demands significantly higher temperatures. At the same time, the Michael reagent formed upon cleavage of C–N1 bond reacts with thymine producing significant amounts of *N*-3 substituted derivatives. Previous theoretical and experimental gas-phase investigations of retro-Michael addition also showed that this reaction is a low barrier process and therefore favorable in the gas-phase regardless of the charge state [20].

Thymine derivatives employed by Walczak and coworkers are structurally similar to our sulfonamidine **II** and, having this in mind, one can ask a question whether there is a significant difference in the fragmentation pattern of the *N*-1 and *N*-3 substituted thymine. Our aim was, therefore, to investigate reactivity of the *N*-1 and *N*-3 subsitututed sulfonamidine in the gas phase and solution. Obtained results will provide useful information that can be used to track these compounds during biological testing. Additionally, observed reactivity of these sulfonamidines will help us to tune desired properties of the second generation sulfonamidine drugs more easily. MS studies were performed in both ES^+ and ES^- modes and the mechanisms of the fragmentations were investigated using DFT methods. Hydrogen/deuterium exchange experiments were performed in order to confirm the number of exchangeable protons and additionally support fragmentation pathways.

Experimental

Preparation of N-Alkyl N-Sulfonylamidino Thymine Derivatives

N-1 substituted thymine **1** [10] was reacted with tetrabutylammonium fluoride (TBAF) in dry THF producing new *N*-3 substituted thymine **5** and *N*-1, *N*-3-disubstituted thymine **4** along with unreacted starting compound **1**. Additionally, acryl sulfonamidine **3** and free thymine **2** were also identified, confirming that the reaction proceeds through the retro-Michael/Michael addition reaction sequence. Details of the reaction are given in Supplemental Material. The reaction products, five well separated spots on silica gel plates, were scraped off and extracted with methanol. The structures of the products were assigned according their ^1H and ^{13}C NMR spectra and additionally confirmed by the ESI-MS^n studies. Both methods proved the presence of the products **1**–**5** in the reaction mixture (Scheme 1, and Supplemental Material, Figures S1–S5).

ESI-MS Analysis

The mass spectral data (ESI-MS and ESI-MS/MS) were acquired on the Agilent 6410 Triple Quad mass spectrometer from Agilent Technologies Inc. (Palo Alto, CA, USA) equipped with electrospray ionization (ESI) interface operated in positive and negative ion mode. The samples were prepared in CH_3OH to a concentration of about 0.05 mg/mL and directly infused. The infusion into the mass spectrometer was performed at a flow rate of 3 μL/min. Nitrogen was used as auxiliary and sheath gas. Spray voltage was set at 4.0 kV, the capillary temperature was 300°C, and the voltage range of the collision cell was 80–180 eV. Full mass spectra were acquired over the mass range *m/z* 10–2000.

MS^n ($n > 2$) were recorded on the amaZon ETD mass spectrometer (Bruker Daltonik, Bremen, Germany) equipped with the standard ESI ion source (Nebulizer pressure: 8 psi; drying gas flow rate: 5 L/min; drying gas temperature: 250°C). The mass spectrometer was operated in positive and negative polarity mode; the potential on capillary cap was ±4500 V. Helium was used as collision gas. The compounds were dissolved in methanol to a concentration of approximately 0.5×10^{-6} mol/dm^3 and injected into the ESI source of the mass spectrometer by syringe pump at a flow rate of 1 μL/min.

Calculation Methods

All calculations were performed by Gaussian09 [21]. Structures of each stationary point along the reaction pathways were optimized at the B3LYP/6-31G(d) level of theory [22–26] and the electronic energies were obtained from the single point

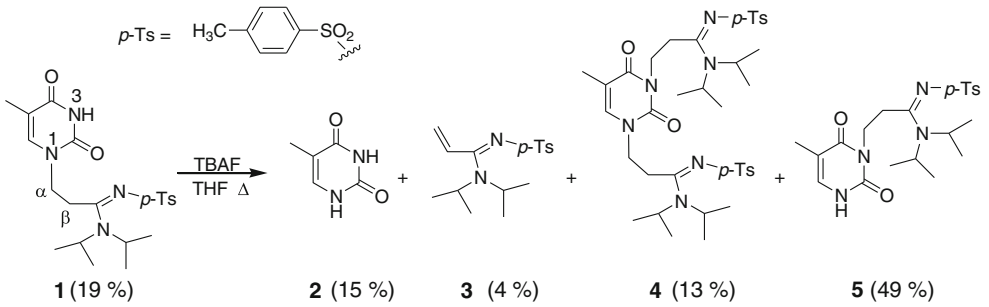

Scheme 1. Reaction of **1** with tetrabutylammonium fluoride (TBAF). Approximate relative abundances (molar ratios) of each compound are given in parentheses

energy calculations using the M06-2X/6-311+G(3df,2p) [27] method. Nature of each stationary point was verified by vibrational analyses (NImag = 0 for minima and NImag = 1 for transition state structures). Correctness of each transition state structure (TS) was confirmed by the intrinsic reaction coordinate following until reactant or product region on the PES was reached without a doubt. Gibbs energies of all molecules were calculated by using thermochemical data directly obtained by calculations without any scaling or corrections for the low vibrations. Structures were visualized and plotted by MOLDEN 5.0 program [28]. All energies are given in kilocalories per mole where 1 kcal = 4.184 kJ.

Results and Discussion

Driven by the results of Walczak and coworkers [19], we decided to investigate the reaction of sulfonamidine **1** (Scheme 1) with fluoride anion as a base. Efficient removal of the arylsulfonyl group from the sulfonamidino compounds by TBAF in THF has been described in literature [29] and, therefore, this reagent was used as a source of fluoride anion expecting amidine deprotection as the significant competitive side-reaction. Using tetrabutlyammonium fluoride (TBAF) [29] to remove the sulfonyl group in **1** gave a complex reaction mixture containing starting material **1**, thymine **2,** and product compounds **3**–**5** (Scheme 1) while no products of desulfonation reaction were found.

Considering the structures of the products, it appears that the fluoride, as a sufficiently strong base in THF, induced elimination of thymine **2**, giving conjugated acryl sulfonamidine **3** as a potential Michael acceptor. The formation of the *N*-1,*N*-3-dialkylated thymine derivative **4** could be explained by the Michael-type addition of starting compounds **1** (F^- assists the creation of N3 anion in **1**) to acrylic derivative **3,** whereas the Michael-type addition of thymine **2** anion to acrylic derivative **3** could lead to the formation of the *N*-1-alkylated **1** and *N*-3-alkylated product **5** as reported for similar alkylation reactions with other pyrimidine derivatives [30, 31]. Observed product composition is in qualitative agreement with the known reactivity of *N*-1 and *N*-3 substituted thymine derivatives [19].

We also wanted to test possibility of S–N bond cleavage in the sulfonamidine **1** under different conditions since this process was identified as one of two dominant processes in the gas phase (see ESI-MS results below). Sulfonyl groups are used to protect amines or other nitrogen containing functionalities and they are difficult to remove under standard hydrolytical conditions [32]. Instead, reductive methods are usually employed, such as the use of sodium amalgam [33, 34], Na-naphthalenide [35–37], or magnesium in methanol [38, 39]. In our hands, application of Na-naphthalenide or magnesium in methanol to remove the sulfonyl group in *N*-1 substituted thymine **1** appeared unsuccessful and mostly the starting material was isolated.

Since the retro-Michael addition was found to be the only process in the solution that encompasses bond cleavage, we conducted a detailed mechanistic investigation of the fragmentation of **1** (*N*-1) and **5** (*N*-3) compounds in

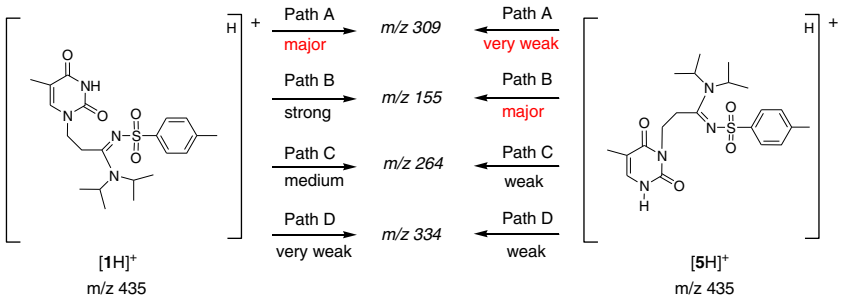

Scheme 2. Product ions obtained via four primary fragmentation pathways starting from signal at *m/z* 435 assigned as $[MH]^+$ adduct of the compounds **1** or **5**. Path D was observed at $E_{lab} \geq 10$ eV. Qualitative description of the intensities is given for the spectra at the collision energy $E_{lab} = 10$ eV

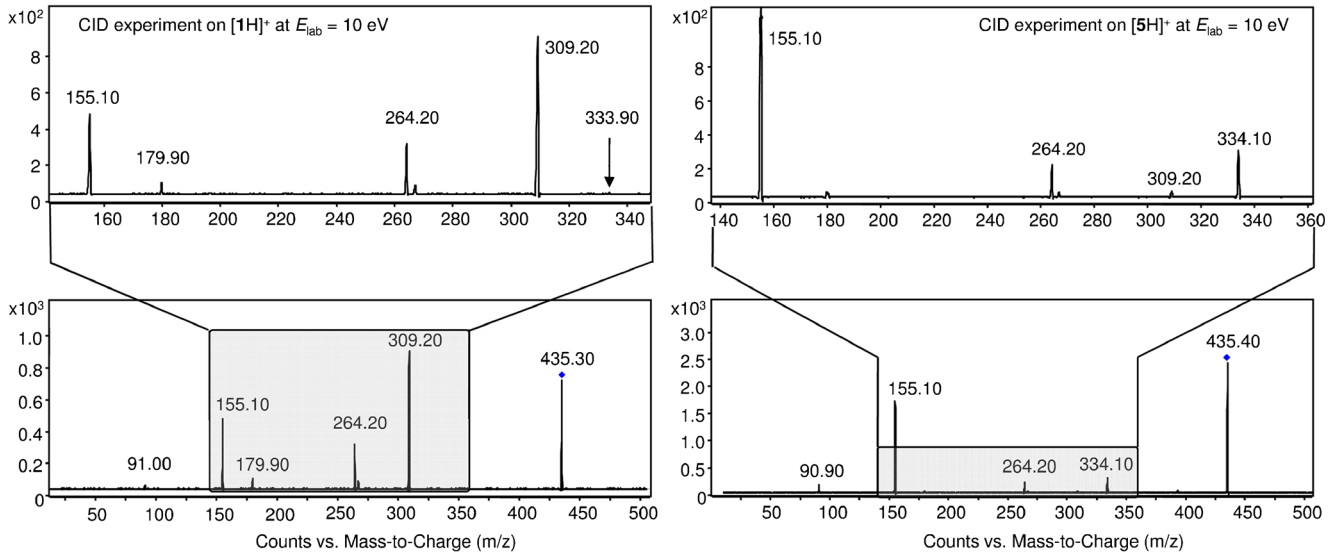

Figure 2. Full (bottom) and stretched out (top) spectra of product ion spectra of the protonated *N*-1 substituted thymine [**1**H]$^+$ and its *N*-3 substituted isomer [**5**H]$^+$ in ES$^+$ mode at the collision energy E_{lab} = 10 eV

order to clarify, understand, and explain the preference of the retro-Michael reaction against other possible fragmentation mechanisms.

ESI MS Results

Transformation of compound **1** (Scheme 1) was studied by ESI, using the ion trap for MS^n studies, and triple-quadrupole for ESI-MS/MS studies. The spectra were obtained at the same concentrations (in MeOH) and conditions in both ES$^+$ and ES$^-$ modes. The fragmentation pathways for all analyzed compounds were proposed based on MS/MS and MS^n spectra of the ions obtained by protonation ([MH]$^+$) or deprotonation ([M–H]$^-$) of the starting molecule.

Our first observation was that *N*-1 substituted thymine **1** and *N*-3 substituted thymine **5** formed protonation products **1**H$^+$

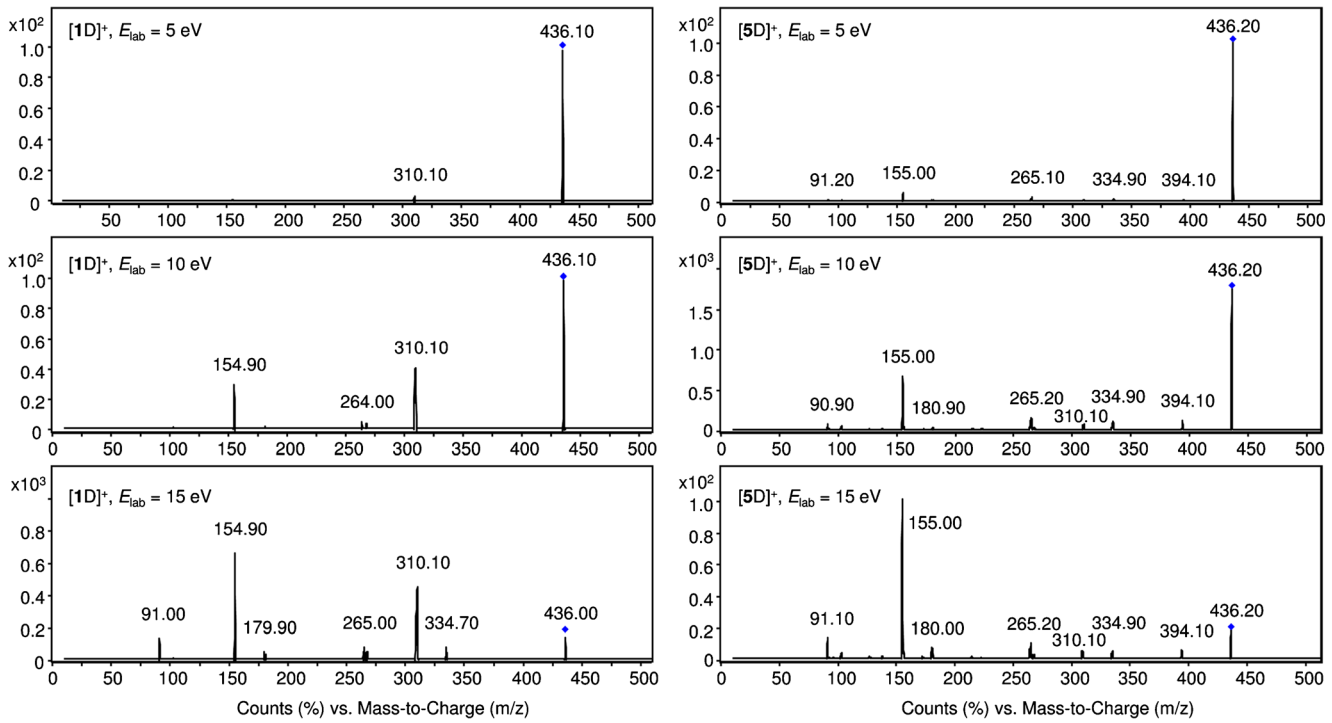

Figure 3. Product ion spectra of the monodeuterated *N*-1 substituted thymine [**1**D]$^+$ and its *N*-3 isomer [**5**D]$^+$ in ES$^+$ mode at E_{lab} = 5, 10 and 15 eV

and $\mathbf{5}H^+$, respectively, as well as several adducts with Na^+ ions in the gas phase with ligand to sodium ratio varying from 1:1 to 4:1. We have noticed that CID experiments conducted on the $[\mathbf{1}H]^+$ and $[\mathbf{1}Na]^+$ produced similar fragmentation scheme. Significant difference between fragmentation patterns starting from **1** (*N*-1) and **5** (*N*-3) has been observed in both positive and negative mode. Although the results obtained in negative mode could be better correlated with our experimental results, we shall start with discussion of the results obtained in positive mode since the differences in fragmentation channels are richer. Four fragmentation channels for compound **1** (*N*-1) were observed and identified in ES^+ mode (Scheme 2) as follows: (1) signal at *m/z* 309 assigned as $[MH]^+$ acryl sulfonamidine **3**, gained because of cleavage of *N*1–CH_2 bond and elimination of thymine base (Path A); (2) signal at *m/z* 155 assigned as $[C_7H_7SO_2]^+$ sulfonyl group (Path B); (3) signal at *m/z* 264 obtained because of elimination of the neutral sulfonamide $[C_7H_7SO_2NH_2]$, (Path C), and (4) signal located at *m/z* 334 corresponding to the elimination of di-isopropylamine (Path D). As it can be seen clearly in Figure 2, the signal at *m/z* 309 assigned as $[MH]^+$ of acryl sulfonamidine **3** is the most abundant in the product ion spectra starting from $[\mathbf{1}H]^+$, whereas signal at *m/z* 155 assigned as $[C_7H_7SO_2]^+$ sulfonyl group (Path B) dominates in the product ion spectra for $[\mathbf{5}H]^+$. It should be noted that the signal at *m/z* 155 is also observed in the spectra of **1** and the relative abundance of this ion is similar in CID product spectra of both *N*-1 and *N*-3 isomers. Several other peaks (*m/z* 266, 222, 180, etc.) are also visible in the CID spectra that are the product ions of two or more consecutive fragmentation processes that have been confirmed by MS^2 and MS^3 experiments (Figures S6 and S7 in Supplemental Material) and mechanisms of their formation will not be discussed any further.

By the increase of the collision energy E_{lab} from 5 to 15 eV, the fragmentation channels starting from $[\mathbf{1}H]^+$ switched priorities and the loss of the tosyl group (Path B, *m/z* 155; at E_{lab}

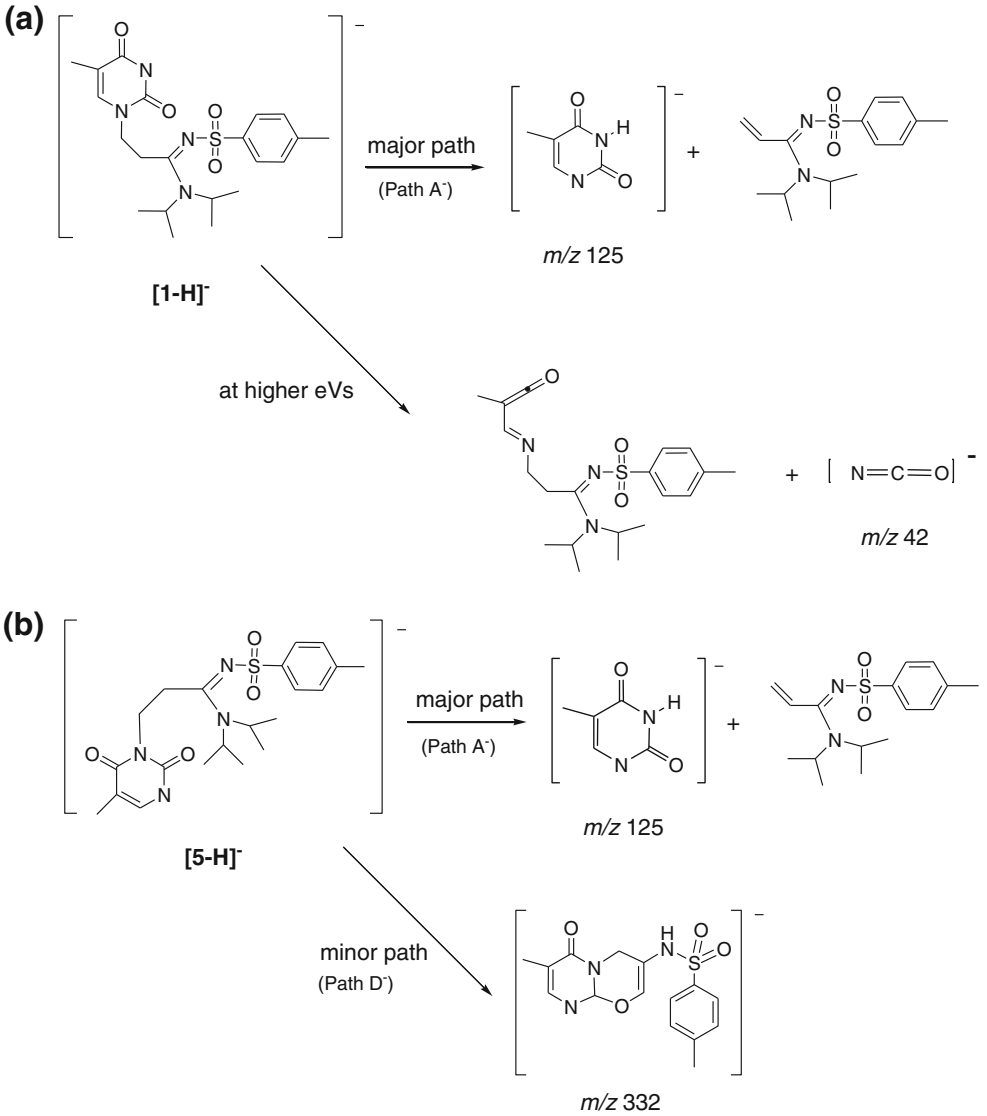

Scheme 3. Proposed structures of signals observed for fragmentation of compounds: a) $[\mathbf{1}\text{-}H]^-$ and b) $[\mathbf{5}\text{-}H]^-$, in ES^- mode

5 eV this signal was below threshold) became the main fragmentation channel (Figure 3 and Figure S8 in Supplemental Materials).

Additionally, H/D exchange experiments were conducted as follows: the samples for H/D exchange were dissolved in D_2O to a concentration of about 0.05 mg/mL and directly infused. In this way, the exchange of the most acidic protons (NH) was expected. Thus, the parent ions $[\mathbf{1}H]^+$ and $[\mathbf{5}H]^+$ showed two additional signals above the threshold of the measurements corresponding to the mono- ($[\mathbf{1}D]^+$ and $[\mathbf{5}D]^+$) and di-deuterated ($[\mathbf{1}D_2]^+$ and $[\mathbf{5}D_2]^+$) ions. The gas fragmentation experiments on these none-, mono- and dideuterated ions showed that the H/D exchange does not affect the fragmentation pattern showing, in the case of $[\mathbf{1}H]^+$, the same switch it the preference of the fragmentation channels upon increase of the collision energy. Fragmentation of both the mono-deuterated ($[\mathbf{1}D]^+$ and $[\mathbf{5}D]^+$) derivatives led to the extrusion of either mono- or non-deuterated thymine (product ions at *m/z* = 309 and 310). Additionally, presence of the product ion with *m/z* 311 in the CID spectra of dideuterated ions ($[\mathbf{1}D_2]^+$ and $[\mathbf{5}D_2]^+$, Figure S8 in Supplementary Material) indicate the presence of the highly enolizable CH hydrogen atoms, which could undergo H/D exchange.

The apparent difference in the fragmentation of *N*-3 substituted $[\mathbf{5}H]^+$ and *N*-1 substituted $[\mathbf{1}H]^+$ is the preferred cleavage of the sulfonic group (*m/z* 155) in the former and the formation of the acryl sulfonamidine $[\mathbf{3}H]^+$ (*m/z* 309) in the latter. This suggests that the substituent at N1 undergoes easier cleavage compared with the N3 substituent. In accord with the latter stands the observation that the fragmentation channels for the protonated *N*-1, *N*-3-disubstituted thymine $[\mathbf{4}H]^+$ show formation of acryl sulfonamidine $[\mathbf{3}H]^+$ by preferred cleavage at the N1 thymine position signifying that the N3–C bond is stronger than the N1–C bond in $[MH]^+$. Afore-mentioned experimental findings observed in the positive mode were rationalized using DFT calculations as discussed in the next section.

A difference in fragmentation of the *N*-3 substituted **5** versus *N*-1 substituted **1** was also observed by the CID experiments in the ES^- mode. Fragmentation of $[\mathbf{1}H]^+$ and $[\mathbf{5}H]^+$ proceeded with few product ions formed (Scheme 3, and Figure S9 in Supplemental Materials).

Retro-Michael addition process leading to the extrusion of free thymine base anion (*m/z* 125) was found to be the dominant reaction channel for both isomeric starting anions (Scheme 3b). This process corresponds to the Path A described also as the most abundant reaction channel for $[\mathbf{1}H]^+$ in positive mode (Scheme 2). To emphasize similarity of these fragmentation paths, we shall term the negative mode path as Path A^-. On the other hand, no N–S bond cleavage products (Path B, Scheme 2) or the sulfonamidine extrusion (Path C, Scheme 2) were obtained upon CID of any of the considered isomeric anions. The low energy product ion spectra of $[\mathbf{5}\text{-}H]^-$ anion in negative mode showed the departure of di-isopropylamine (Scheme 3b), as the minor process with the ca 30% abundance relative to the Path A^-. The same was not observed in CID experiments conducted on $[\mathbf{1}\text{-}H]^-$. It should be mentioned that the product ions spectra for $[1\text{-}H]^-$ also showed departure of NCO^- (*m/z* 42) as the minor path at higher collision energies (Scheme 3a). Appearance of NCO^- fragment in the negative mode CID spectra of the ion $[\mathbf{1}\text{-}H]^-$ indicates substitution position, additionally confirming the structure of the starting ion [40]. This could be rationalized by analogy to the fragmentation of a thymine anion. Thymine N1-H deprotonation led to an anion, which was stabilized by resonance through the ring where O4 accepted charge what was confirmed by the N1-H acidity decrease in O4 substituted derivative, Scheme 3 [41]. Owing to the higher gas-phase acidity (GA) of N1-H compared with N3-H the corresponding anion with the charge located on N1 is more stable and ring cleavage does not proceed through deprotonation at N1. In line with this, the fragmentation of $[\mathbf{5}\text{-}H]^-$ did not show formation of NCO^- fragment even under the higher energy CID conditions. Our results agree well with previous experimental and theoretical results for thymine, *N*-1-methylthymine, *N*-3-methylthymine, *O*-2-methylthymine, and *O*-4-methylthymine [42].

Calculation Results

To explain the observed fragmentation patterns in positive and negative mode described in the previous section, we calculated reaction Gibbs energies ($\Delta_r G$) and the activation energies (E_a) for the primary reaction pathways leading to a fragmentation of the starting ion into two fragments. Again, we shall start our discussion by analyzing the reaction paths at the cationic potential energy surface. Optimized structure of the starting ion $[\mathbf{1}H]^+$ is presented in Figure 4.

Apart from Path B, all other observed processes are initiated by the H_β proton shifts to either thymine subunit (Path A) or toward one of the amidine nitrogen atoms (N_{SA} or N_{iPr}, Paths C and D, respectively, structures **9** or **12** in Scheme 4), and our

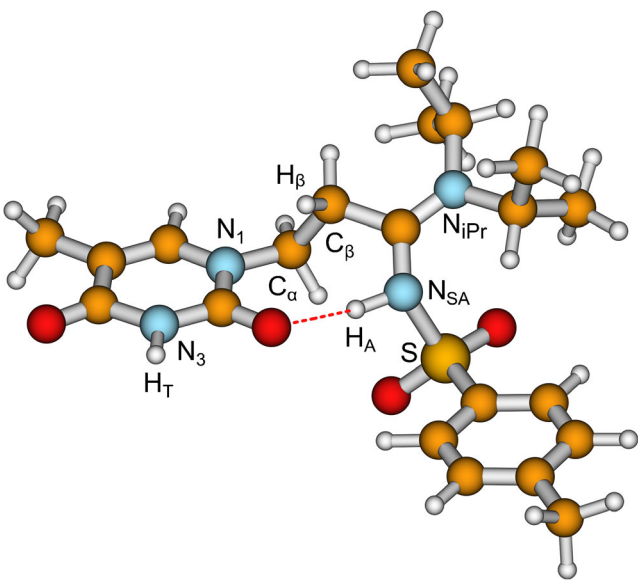

Figure 4. Optimal structure of the protonated *N*-1 substituted thymine **1H⁺** calculated at B3LYP/6-31G(d) level of theory

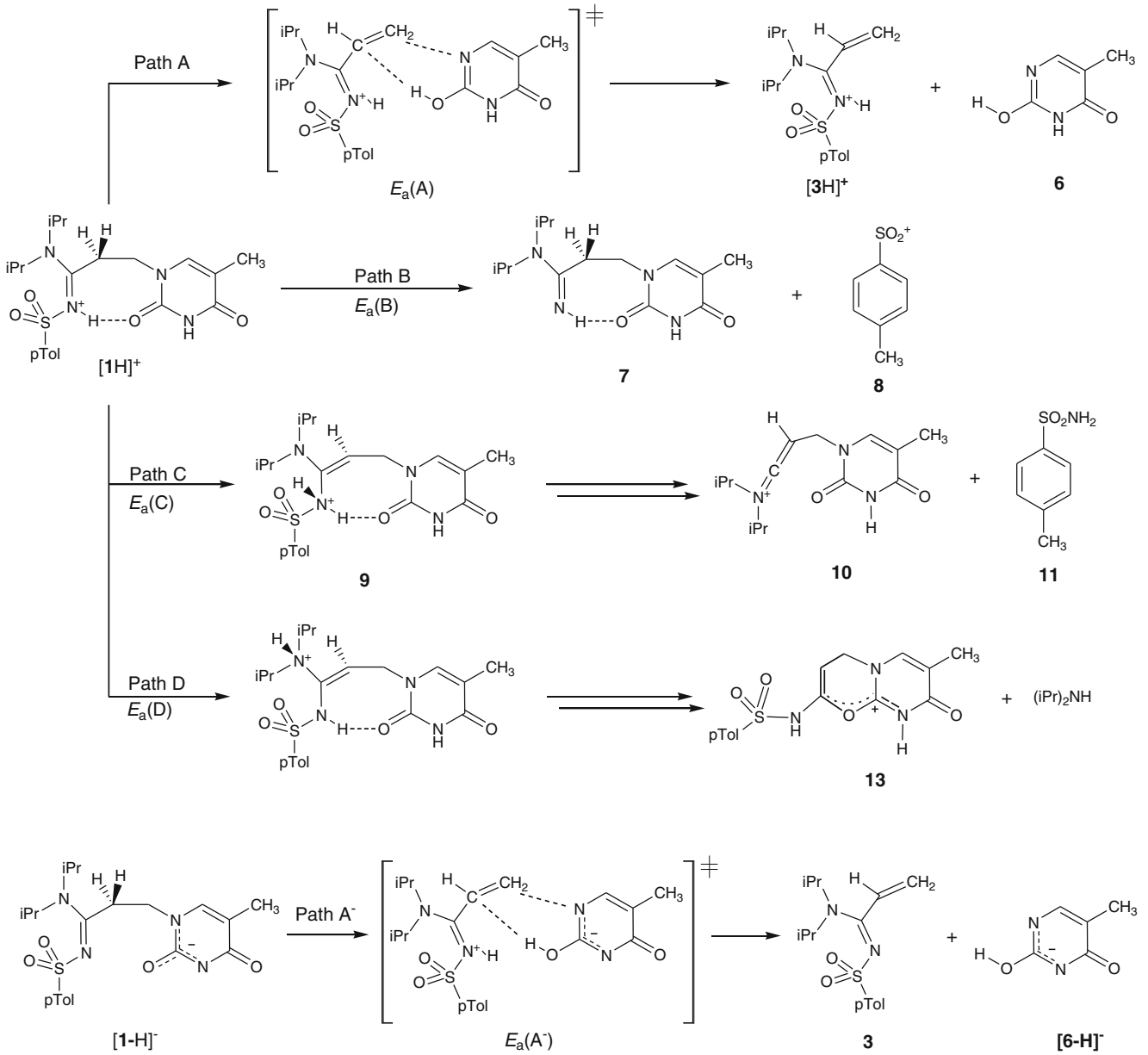

Scheme 4. Schematic representation of four investigated fragmentation paths starting from the *N*-1 isomer $[\mathbf{1}H]^+$ and the McLafferty-type fragmentation path (Path A^-) starting from the anion $[\mathbf{1}\text{-}H]^-$

calculations predict that these proton shifts are the rate-determining steps along the corresponding reaction paths. In the case of Path B, fragmentation proceeds by direct S–N_{SA} bond cleavage without any proton shift associated with this process.

The lowest energy transition state structures calculated for all four primary fragmentation paths are shown in Figure 5, and the structures of the cumulative results of kinetic and thermodynamic investigations of the four fragmentation pathways are shown in Table 1.

Locating a minimum energy reaction path for Path A appeared to be the most demanding task. Four different routes were found, each of them initiated by a proton shift from ethyleneamidine moiety toward thymine subunit.

The McLafferty type of fragmentation was found to be kinetically favorable over the other tested mechanisms (see Supplemental Materials, Figure S11). This mechanism includes H_β proton shift to one of the neighboring oxygen atoms in a 1,5-fashion inducing N1(N3)–C_α bond scission and proceeding further to the products through the formation of the six-membered transition state (TS_A, Figure 5). A six-membered cyclic transition state can also be formed by the amidine proton shift toward N1, which would also lead to the N1–C_α bond scission. However, the barrier calculated for this process is significantly higher (63.8 and 72.7 kcal mol^{-1} in $[\mathbf{1}H]^+$ and $[\mathbf{5}H]^+$, respectively; see Supplemental Material, Figure S11). The reason for this lies in a direct formation of the acrylic double bond in the McLafferty type of rearrangement, whereas

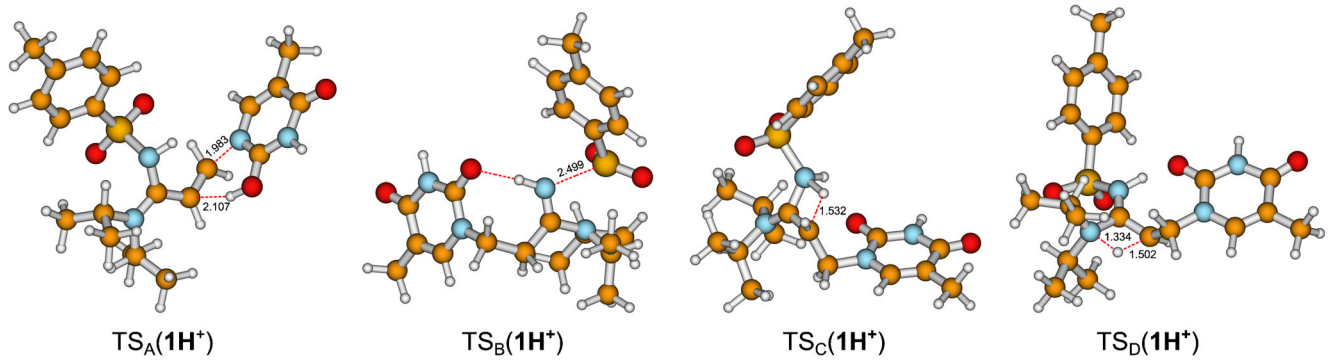

Figure 5. Optimized transition state structures for the fragmentation paths A-D of *N*-1 substituted derivative [**1**H]$^+$

in the case of amidine (NH) proton migration, unstable primary carbocation needs to be formed. Another considered possibility was H_β-to-N1 1,3-proton shift, which would also lead to a direct formation of acrylic bond. Such reaction involves the tight four-membered transition state, which is connected to the relatively high activation energy (see Supplemental Materials, Figure S11). The fourth possibility is direct C–N1(N3) bond cleavage, which ends up in formation of the four-membered ring instead of acrylamidine. Calculated barrier of 77.3 kcal mol^{-1} for [**1**H]$^+$ (72.3 kcal mol^{-1} for [**5**H]$^+$) for this process also rules it out as the least favorable possibility.

Our calculations indicate that migration of the same H_β proton also triggers Paths C and D (Scheme 4 and TS$_C$ and TS$_D$ in Figure 5) where 1,3-proton shift toward either of two amidine nitrogen atoms leads to a formation of the less stable intermediates **9** and **12** (Scheme 4), which undergo extrusion of the neutral sulfonamide or diisopropylamine in the energetically favorable processes. Again, an alternative pathway for a migration of the proton suited at thymine subunit (H_T, Figure 4) toward the amidine group was tested. This pathway involves a three-step process in which carbonyl oxygen serves as a mediator for the proton shift (see Supplemental Material Figure S12). The latter mechanism is calculated to have a slightly higher barrier (75.7 kcal mol^{-1} in the case of *N*-1 derivative) than H_β proton shift. Thus, the one-step H_β proton shift is considered to be more probable if compared with the three-step alternative. Finally, extrusion of the tolylsulfonyl cation **8** (Path B in Scheme 5 and TS$_B$ in Figure 5) is a consequence of direct N–S bond cleavage and is not activated by any proton shift.

In the case of *N*-1 derivative, experimentally observed results agree well with the trend in the calculated activation energies. Activation energy for the fragmentation via Path A is the lowest one and consequently it is the most populated fragmentation channel. According to the calculations, Path B is disfavored with respect to Path A by 13.5 and 6.4 kcal mol^{-1} for *N*-1 and *N*-3 derivative, respectively. A smaller difference in the activation energy is apparently sufficient to induce a switch in the preference of the fragmentation channels and an almost complete retardation of Path A. A fragmentation via the Path B arises from a simple stretching of the sulfonamide N–S bond and does not require to be activated by the proton shift. Such processes usually occur through a late transition state possessing large density of states. Consequently, these fragmentation channels can be preferred regardless of their higher activation energies [43].

Paths C and D are strongly disfavored over Paths A and B because of their high activation energies (ca 70 kcal mol^{-1}). This is particularly true for the extrusion of diisopropylamine (Path D), which starts to appear at higher collision energies with respect to other paths as commented earlier in the text. However, a slightly higher abundance of Paths C and D over Path A (Figure 2) in the case of the *N*-3 isomer is still surprising and may indicate another channel leading to the loss of the signal with *m/z* = 309. Indeed, fragmentation of the signal with *m/z* = 309 led to desulfonation of the amidine group producing dominantly an ion with *m/z* = 155 (Figure S6 in Suppl. Mat.) which, in conjunction with higher barrier for the Path A, could be responsible for the very weak intensity of [**3**H]$^+$ in the product ion spectra of [**5**H]$^+$.

Finally, a brief analysis of the Path A$^-$ on the anionic potential energy surface was done. McLafferty-like transition state analogous to the one found for the positive mode fragmentation was identified. The calculations predict the even lower activation energies amounting to 26 and 34 kcal mol^{-1}

Table 1. Activation Energies (E_a) of the Rate-Determining Reaction Steps and the Gibbs Energies for the Overall Fragmentation Process ($\Delta_r G$) Along the Investigated Fragmentation Paths[a,b]

	Precursor ions: [**1**H]$^+$ or [**1**-H]$^-$		Precursor ions: [**5**H]$^+$ or [**5**-H]$^-$	
Paths	E_a(Path)	$\Delta_r G$(Path)	E_a(Path)	$\Delta_r G$(Path)
A	35.5	17.7	41.4	28.9
B	49.0	62.3	48.0	65.3
C	69.2	20.4	71.3	20.7
D	74.3	31.8	76.9	34.9
A$^-$	26.0	19.7	33.9	28.1

[a]All energies are given in kcal mol^{-1} and were calculated using M06-2X/6-311+G(3df,2p) //B3LYP/6-31G(d) level of theory

[b]Structures of the precursor ions [**1**H]$^+$ and [**1**-H]$^-$, their product ions, and calculated intermediates along the investigated reaction paths are schematically presented in Scheme 4 whereas the corresponding structures derived from [**5**H]$^+$ and [**5**-H]$^-$ are given in Scheme S1 in the Supplemental Material. Complete energy profiles for the fragmentation processes are given in Figure S10 in Supplemental Material

for *N*-1 and *N*-3 isomers, respectively. Difference in the activation energies of 8 kcal mol^{-1} is also higher than the corresponding difference obtained for the same processes in the positive mode. In the negative mode, no mobile protons were present at either thymine or amidine subunits, additionally supporting our finding that shift of H_β proton actually triggers the elimination of thymine. It is reasonable to assume that the presence of base additionally promotes the mobility of H_β proton, leading to the further lowering of the barrier in the basic solution. These findings are in full accordance with the experiment in solution conducted in this work (Scheme 1) and explain strong preference of the retro-Michael reaction over desulfonation and other fragmentation reactions.

Conclusions

Our investigations show that the *N*-1 and *N*-3 tolylsulfonamidino substituted thymine derivatives show significant difference in fragmentation patterns and could be easily differentiated under ESI-MS/MS conditions. Thus, ESI-MS experiments conducted on the *N*-1 derivative showed elimination of acrylamidine (retro-Michael addition) as the most abundant reaction channel in the gas phase under applied conditions. Besides other less important fragmentation pathways, elimination of the sulfonyl group proved to be a competitive process in the positive mode but only under higher energy conditions. On the other hand, *N*-3 derivative **5** is found to be more inert toward the elimination of acrylamidine, which is ascribed to a stronger N–C_α bond and somewhat higher barrier. In this case, removal of the sulfonyl group was found to be a dominant process. Detailed quantum chemical investigations of the observed processes in the gas-phase reveal H(C_β) proton as sufficiently labile, triggering most of the observed primary fragmentation paths. This is particularly true for the formation of acryl sulfonamidine **3**, which is formed in a kinetically favorable process via six-membered McLafferty type transition state. Our calculations also reveal that the same process proceeds even more easily on the anionic potential energy surface, thus providing a basis for explanation of the experimental results. In contrast to the situation in alkyl sulfonamides, reaction channel leading to the elimination of the tolylsulfonamide (Path C) was found to be less populated than the one producing sulfonyl cation (Path B). According to the theoretical and experimental investigations in the gas phase, formed *N*-3 derivative **5** is less prone to the C–N bond cleavage with respect to the derivative **1**. A significant difference in the observed fragmentation pattern of *N*-1 and *N*-3 isomers proves the ESI-MS technique as an excellent method for tracking the fate of similar sulfonamidine drugs during the applications.

The mass spectral results are in a good agreement with the experiments in solution conducted in this work, where the reaction of *N*-1-alkyl-*N*-sulfonylamidino thymine **1** with F^- (TBAF) in THF proceeded by the cleavage of thymine N1–CH_2 bond resulting in the formation of the mixture of the products identified as the *N*-3 substituted thymine **5**, the *N*-3,*N*-1-disubstituted thymine **4**, acryl sulfonamidine **3**, thymine **2**, and starting *N*-1 substituted thymine **1** as a result of the Michael/retro-Michael addition reactions. On the other hand, expected removal of the sulfonyl group from the amidine nitrogen atom was not obtained. The observed in situ *N*-1 and/or *N*-3 thymine alkylation with reactive acryl sulfonamidine **3** as the Michael acceptor may open interesting possibilities for the preparation of other *N*-3 substituted pyrimidines.

Acknowledgments

This work was supported by the Ministry of Science, Education, and Sports of the Republic of Croatia through grants no. 098-0982914-2935; 053-0982914-2965; 098-0982915-2945. Z.G. and B.K. gratefully acknowledge support of the Computing Center of the University of Zagreb (SRCE) for granting computational time on ISABELLA cluster.

References

1. Žinić, B., Žinić, M., Krizmanić, I.: Synthesis of the sulfonylpyrimidine derivatives with anticancer activity. EP 0 877 022 B1 (2003)
2. Supek, F., Kralj, M., Marjanović, M., Šuman, L., Šmuc, T., Krizmanić, I., Žinić, B.: Atypical cytostatic mechanism of *N*-1-sulfonylcytosine derivatives determined by in vitro screening and computational analysis. Investig. New Drugs **26**, 97–110 (2008)
3. Pavlak, M., Stojković, R., Radačić-Aumiler, M., Kašnar-Šamprec, J., Jerčić, J., Vlahović, K., Žinić, B., Radačić, M.: Antitumor activity of novel *N*-sulfonylpyrimidine derivatives on the growth of anaplastic mammary carcinoma in vivo. J. Cancer Res. Clin. Oncol. **131**, 829–836 (2005)
4. Kašnar-Šamprec, J., Ratkaj, I., Mišković, K., Pavlak, M., Baus-Lončar, M., Kraljević Pavelić, S., Glavaš-Obrovac, L., Žinić, B.: In vivo toxicity study of *N*-1-sulfonylcytosine derivatives and their mechanisms of action in cervical carcinoma cell line. Investig. New Drugs **30**, 981–990 (2012)
5. Greenhill, J.V., Lue, P.: Amidines and guanidines in medicinal chemistry. Prog. Med. Chem. **30**, 203–326 (1993)
6. Panico, A., Vicini, P., Incerti, M., Cardile, V., Gentile, B., Ronsisvalle, G.: Amidinobenzisothiazole derivatives with antidegenerative activity on cartilage. Il Farmacol **57**, 671–675 (2002)
7. Bielawski, K., Bielawska, A., Sosnowska, K., Miltyk, W., Winnicka, K., Palka, J.: Novel amidine analogue of melphalan as a specific multifunctional inhibitor of growth and metabolism of human breast cancer cells. Biochem. Pharmacol. **72**, 320–331 (2006)
8. Stolić, I., Mišković, K., Piantanida, I., Baus Lončar, M., Glavaš-Obrovac, L., Bajić, M.: Synthesis, DNA/RNA affinity and antitumour activity of new aromatic diamidines linked by 3, 4-ethylenedioxythiophene. Eur. J. Med. Chem. **46**, 743–755 (2011)
9. Wilson, W.D., Tanious, F.A., Mathis, A., Tevis, D., Hall, J.E., Boykin, D.W.: Antiparasitic compounds that target DNA. Biochimie **90**, 999–1014 (2008)
10. Krstulović, L., Ismaili, H., Bajić, M., Višnjevac, A., Glavaš-Obrovac, L., Žinić, B.: Synthesis of novel aliphatic N-sulfonylamidino thymine derivatives by Cu(I)-catalyzed three-component coupling reaction. Croat. Chem. Acta **85**, 525–534 (2012)
11. Tiller, P.R., Land, A.P., Jardine, I., Murphy, D.M., Sozio, R., Ayrton, A., Schaefer, W.H.: Application of liquid chromatography-mass spectrometry analyses to the characterization of novel glyburidemetabolites formed in vitro. J. Chromatogr. A **794**, 15–25 (1998)
12. Volmer, D.A.: Multiresidue determination of sulfonamide antibiotics in milk by short-column liquid chromatography coupled with electrospray ionization tandem mass spectrometry. Rapid Commun. Mass Spectrom. **10**, 1615–1620 (1996)
13. Hu, N., Liu, P., Jiang, K., Zhou, Y., Pan, Y.: Mechanism study of SO_2 elimination from sulfonamides by negative electrospray ionization mass spectrometry. Rapid Commun. Mass Spectrom. **22**, 2715–2722 (2008)

14. Xu, G., Huang, T., Zhang, J., Huang, J.K., Carlson, T., Miao, S.: Investigation of collision-induced dissociations involving odd-electron ion formation under positive electrospray ionization conditions using accurate mass. Rapid Commun. Mass Spectrom. **24**, 321–327 (2010)
15. Sun, M., Dai, W., Liu, D.Q.: Fragmentation of aromatic sulfonamides in electrospray ionization mass spectrometry: elimination of SO_2 via rearrangement. J. Mass Spectrom. **43**, 383–393 (2008)
16. Wang, Z., Hop, C.E.C.A., Mi-Sook, K., Huskey, S.-E.W., Baillie, T.A., Guan, Z.: The unanticipated loss of SO_2 from sulfonamides in collision-induced dissociation. Rapid Commun. Mass Spectrom. **17**, 81–86 (2003)
17. Hibbs, J.A., Jariwala, F.B., Weisbecker, C.S., Attygalle, A.B..: Gas phase fragmentations of anions derived from *N*-phenyl benzenesulfonamides. J. Am. Soc. Mass Spectrom. **24**, 1280–1287 (2013)
18. Bialecki, J.B., Weisbecker, C.S., Attygalle, A.B..: Low-energy collision-induced dissociation mass spectra of protonated *p*-toluenesulfonamides derived from aliphatic amines. J. Am. Soc. Mass Spectrom. **25**, 1068–1078 (2014)
19. Boncel, S., Maczka, M., Walczak, K.Z.: Michael versus retro-Michael reaction in the regioselective synthesis of *N*-1 and *N*-3 uracil adducts. Tetrahedron **66**, 8450–8457 (2010)
20. Wang, H.-Y., Zhang, X., Guo, Y.-L., Lu, L.: Mass spectrometric studies of the gas phase retro-Michael type fragmentation reactions of 2-hydroxybenzyl-*N*-pyrimidinylamine derivatives. J. Am. Soc. Mass Spectrom. **16**, 1561–1573 (2005)
21. Kitao, O., Nakai, H., Vreven, T., Montgomery Jr., J.A., Peralta, J.E., Ogliaro, F., Bearpark, M., Heyd, J.J., Brothers, E., Kudin, K.N., Staroverov, V.N., Kobayashi, R., Normand, J., Raghavachari, K., Rendell, A., Burant, J.C., Iyengar, S.S., Tomasi, J., Cossi, M., Rega, N., Millam, J.M., Klene, M., Knox, J.E., Cross, J.B., Bakken, V., Adamo, C., Jaramillo, J., Gomperts, R., Stratmann, R.E., Yazyev, O., Austin, A.J., Cammi, R., Pomelli, C., Ochterski, J.W., Martin, R.L., Morokuma, K., Zakrzewski, V.G., Voth, G.A., Salvador, P., Dannenberg, J.J., Dapprich, S., Daniels, A.D., Farkas, Ö., Foresman, J.B., Ortiz, J.V., Cioslowski, J., Fox, D.J.: Gaussian 09, Revision A.1. Gaussian, Inc, Wallingford (2009)
22. Ditchfield, R., Hehre, W.J., Pople, J.A.: Self-consistent molecular-orbital methods. IX. An wxtended Gaussian-type basis for molecular-orbital studies of organic molecules. J. Chem. Phys. **54**, 724–728 (1971)
23. Hehre, W.J., Ditchfield, R., Pople, J.A.: Self-consistent molecular orbital methods. XII. Further extensions of Gaussian-type basis sets for use in molecular orbital studies of organic molecules. J. Chem. Phys. **56**, 2257–2261 (1972)
24. Francl, M.M., Pietro, W.J., Hehre, W.J., Binkley, J.S., Gordon, M.S., DeFrees, D.J., Pople, J.A.: Self-consistent molecular orbital methods. XXIII. A polarization-type basis set for second-row elements. J. Chem. Phys. **77**, 3654–3665 (1982)
25. Clark, T., Chandrasekhar, J., Spitznagel, G.W., Schleyer, P.V.R.: Efficient diffuse function-augmented basis-sets for anion calculations. 3. The 3-21+G Basis Set for 1st-row Elements, Li-F. J. Comput. Chem. **4**, 294–301 (1983)
26. Frisch, M.J., Pople, J.A., Binkley, J.S.: Self-consistent molecular orbital methods 25. Supplementary functions for Gaussian basis sets. J. Chem. Phys. **80**, 3265–3269 (1984)
27. Zhao, Y., Truhlar, D.G.: The M06 suite of density functionals for main group thermochemistry, thermochemical kinetics, noncovalent interactions, excited states, and transition elements: two new functionals and systematic testing of four M06-class functionals and 12 other functionals. Theor. Chem. Accounts **120**, 215–241 (2008)
28. Schaftenaar, G., Noordik, J.H.: Molden: A Pre- and post-processing program for molecular and electronic structures. J. Comput. Aided Mol. Des. **14**, 123–134 (2000)
29. Yasuhara, A., Sakamoto, T.: Deprotection of *N*-sulfonyl nitrogen-heteroaromatics with tetrabutylammonium fluoride. Tetrahedron Lett. **39**, 595–596 (1998)
30. Boncel, S., Gondela, A., Walczak, K.: Uracil as a target for nucleophilic and electrophilic reagents. Curr. Org. Synth. **5**, 365–396 (2008)
31. Boncel, S., Walczak, K.: The Influence of base on regioselectivity of 5-substituted uracils addition to michael acceptors. Lett. Org. Chem. **3**, 534–538 (2006)
32. Green, T.W., Wuts, P.G.M.: Protective Groups in Organic Synthesis, pp. 604–607; 744–747. Wiley-Interscience, New York (1999)
33. Ranganathan, R., Larwood, D.: Facile conversion of adenosine into new 2′-substituted-2′-deoxy-arabinofuranosyladenine derivatives: stereospecific syntheses of 2′-azido-2′-deoxy- 2′-amino-2′-deoxy-, and 2′-mercapto-2′-deoxy-β-D-arabinofuranosyladenines. Tetrahedron Lett. **19**, 4341–4344 (1978)
34. Tanner, D., Ming, H.H., Bergdahl, M.: Stereo-controlled synthesis of the spirocyclic alkaloid (±)-nitramine. Tetrahedron Lett. **29**, 6493–6496 (1988)
35. Suzuki, H., Unemoto, M., Hagiwara, M., Ohyama, T., Yokoyama, Y., Murakami, Y.: Synthetic studies on indoles and related compounds. Part 46.1 First total syntheses of 4,8-dioxygenated β-carboline alkaloids. J. Chem. Soc. Perkin Trans. **1**, 1717–1724 (1999)
36. Ji, S., Gortler, L.B., Waring, A., Battisti, A.J., Bank, S., Closson, W.D., Wriede, A.P.: Cleavage of sulfonamides with sodium naphthalene. J. Am. Chem. Soc. **89**, 5311–5312 (1967)
37. Yoo, E.J., Bae, I., Cho, S.H., Han, H., Chang, S.: A Facile access to *N*-sulfonylimidates and their synthetic utility for the transformation to amidines and amides. Org. Lett. **8**, 1347–1350 (2006)
38. Sridhar, M., Kumar, B.A., Narender, R.: Expedient and simple method for regeneration of alcohols from toluenesulfonates using Mg-MeOH. Tetrahedron Lett. **39**, 2847–2850 (1998)
39. Murase, M., Watanabe, K., Yoshida, T., Tobinaga, S.: A new concise synthesis of arcyriacyanin A and its unique inhibitory activity against a panel of human cancer cell line. Chem. Pharm. Bull. **48**, 81–84 (2000)
40. Bald, I., Flosadóttir, H.D., Ómarsson, B., Ingólfsson, O.: Metastable fragmentation of a thymidine-nucleotide and its components. Int. J. Mass Spectrom. **313**, 15–20 (2012)
41. Tehrani, Z.A., Fattahi, A.: Comparison of gas phase intrinsic properties of cytosine and thymine nucleobases with their *O*-alkyl adducts: different hydrogen bonding preferences for thymine versus *O*-alkyl thymine. J. Mol. Model. **8**, 2993–3005 (2013)
42. Kurinovich, M.A., Lee, J.K.: The acidity of uracil and uracil analogs in the gas phase: four surprisingly acidic sites and biological implications. J. Am. Soc. Mass Spectrom. **13**, 985–995 (2002)
43. Vekey, K.: Internal energy effects in mass spectrometry. J. Mass Spectrom. **31**, 445–463 (1996)